ETH
Eidgenössische Technische Hochschule Zürich
Swiss Federal Institute of Technology Zurich

Well-balanced methods for computation of the standing accretion shock instability (SASI)

Master Thesis

Samuel Maloney

December 14, 2018

Advisors: Prof. Dr. Siddhartha Mishra, Dr. Roger Käppeli

Department of Mathematics, Seminar for Applied Mathematics, ETH Zürich

Abstract

Simulating the standing accretion shock instability.

Contents

Chapter 1

Introduction

In the study of astrophysical entities, accretion shocks are a fairly commonly encountered physical phenomena. In particular, standing accretion shocks (SAS) are part of the theory behind core-collapse supernovae, with an instability (SASI) described by Blondin et al. [1] being proposed as a possible mechanism for driving the explosive evolution of these phsyical systems. This instability occurs because of the spherical nature of the system, with the effects of perturbations to the symmetry of the shock being trapped in the interior subsonic region and producing feedback loops which further perturb the shock front.

To gain a better understanding of the underlying mechanisms of this instability, Foglizzo [2] and Sato et al. [3] (hereafter referred to together as FS) proposed and studied a simple toy problem, the details of which are presented in Section 2.2. Using this simple set-up they showed evidence for a coupled advective-acoustic cycle between the stationary shock front and an interior decelerating potential step that is intended to model the effects of matter settling onto the surface of the accreting object.

For this thesis, well-balanced methods for simulating steady states in the presence of external potential fieds, as developed by Käppeli and Mishra [4] (hereafter referred to as KM), were applied to the aforementioned toy problem as well as 2D simulations of the SASI scenario using circular and spherical geometries. The mathematical theory of fluid flow and associated steady states is briefly outlined in Section 1.1 while an overview of the numerical method and well-balanced scheme used for this thesis is given in Section 1.2.

1.1 Euler Equations

The time evolution of the dynamics of fluids can be described by systems of balance laws. For inviscid fluids, this system is given by the well-known Eu-

ler equations with source terms, which mathematically represent the physical conservation of mass, momentum, and energy. They are given here following the notation of KM as

$$\frac{\partial \rho}{\partial t} + \nabla \cdot (\rho \mathbf{v}) = 0, \tag{1.1a}$$

$$\frac{\partial \rho \mathbf{v}}{\partial t} + \nabla \cdot (\mathbf{v} \rho \mathbf{v}) + \nabla p = -\rho \nabla \phi, \tag{1.1b}$$

$$\frac{\partial E}{\partial t} + \nabla \cdot [(E + p)\mathbf{v}] = -\rho \mathbf{v} \cdot \nabla \phi, \tag{1.1c}$$

where ρ is the mass density, and $\mathbf{v}$ is the local velocity vector. E is the total energy sum of the internal and kinetic energies given as

$$E = \rho e + \frac{\rho \mathrm{v}^2}{2}. \tag{1.2}$$

An equation of state $p = p(\rho, e)$ must be selected for a given problem to complete the relations between these primitive quanitites. The quantitiy ϕ on the right-hand side of the latter two equations represents an external potential field (e.g. gravity) which acts upon the fluid. For our purposes, this potential is assumed to be known, either as a given value, through precomputation, or by solving for it independently of the other fluid quantities at each time step.

The Euler system of equations can be rewritten in the condensed form of a general balance law as

$$\mathbf{U}_t + \nabla \cdot (\mathbf{F}(\mathbf{U})) = \mathbf{S}(\mathbf{U}), \tag{1.3}$$

where $\mathbf{U}$ is a vector of the conserved quantities, and $\mathbf{F}$ and $\mathbf{S}$ represent the fluxes and sources of these quanitites in the system.

1.1.1 Steady States

For fluid flows in the presence of an external potential field, non-trivial steady states (also called stationary solutions) can arise. Highly accurate simulations of these stationary solutions are of interest as they allow for accurate reproduction and analysis of subsequent perturbations to the system, which can be quite small and therefore overwhelmed by the truncation error of a less well-resolved scheme.

It can be seen that for a steady state solution the time derivative term is exactly zero and the balance law (1.3) reduces to a balance between the fluxes and sources as

$$\nabla \cdot (\mathbf{F}(\mathbf{U})) = \mathbf{S}(\mathbf{U}). \tag{1.4}$$

In order to reach a unique solution to this balance, some constraint on the thermodynaomics of the system must be specified. Several options are

possible depending on the flow scenario to be modelled, with two important classes comprising constant entropy and constant temeprature flows, i.e. isentropic and isothermal flows, respectively.

For example, Bernoulli's principle gives us that the following quantiity should remain constant along streamlines of an isentropic steady flow

$$\frac{\mathrm{v}^2}{2} + \phi + h = \text{constant} \equiv b \tag{1.5}$$

where b is referred to as the Bernoulli constant and h is the specific enthalpy

$$h = e + \frac{p}{\rho}. \tag{1.6}$$

This constancy can then be leveraged in a computational scheme to find the unique weak solution for such an isentropic flow.

1.2 Numerical Methods

It is well-studied that the non-linear nature of the Euler equations (1.1) can lead to very complicated flow features, such as turbulence and shocks, even from initially smooth conditions. As such, numerical solutions to these systems can only be found in a weak sense and require some other thermodynamic information, e.g. regarding the entropy or temperature, in order to fix a unique solution. Many methods have therefore been developed to resolve such flows in a stable and consistent manner, with the class of finite volume methods (FVM) being one of the most popular for conservation laws.

1.2.1 Spatial Discretization

Starting in one dimension for simplicity, the Euler equations in the balance law form (1.3) reduce to

$$\frac{\partial \mathbf{U}}{\partial t} + \frac{\partial \mathbf{F}}{\partial x} = \mathbf{S}, \tag{1.7}$$

where the vectors of conserved quanitites, and their fluxes and sources are respectively defined as

$$\mathbf{U} = \begin{bmatrix} \rho \\ \rho \mathrm{v}_x \\ E \end{bmatrix}, \quad \mathbf{F} = \begin{bmatrix} \rho \mathrm{v}_x \\ \rho \mathrm{v}_x^2 + p \\ (E+p)\mathrm{v}_x \end{bmatrix}, \quad \mathbf{S} = \begin{bmatrix} 0 \\ -\rho \\ -\rho \mathrm{v}_x \end{bmatrix} \frac{\partial \phi}{\partial x}. \tag{1.8}$$

It is also useful to define a vector of primitive variables $\mathbf{w} = [p,\ \mathbf{v},\ T]^T$. While the methods used here are generally applicable to any choice of the equation of state, the ideal gas law will be assumed here as an example for the derivations. It is given by

$$p = \rho e(\gamma - 1), \tag{1.9}$$

where the adiabatic index $\gamma = C_p/C_v$ is the ratio of specific heats at constant pressure and volume, respectively.

A typical FVM discretizes the domain into small cells (i.e. volumes) and then evolves the cell averages of the conserved quantities by computing their fluxes at all of the faces between adjacent volumes. As the values in adjacent cells differ in general, a Riemann problem will appear at each cell interface which can then be solved to obtain the fluxes. Exact solutions are possible and are the basis of the so-called Godunov schemes [5], but usually the computational effort is saved by using an approximate solution, such as from a Roe [6], Rusanov [7], or HLLC [8] solver, as the rest of the method is itself only approximate due to truncation error.

1.2.2 Well-Balanced Reconstruction

Up to second-order accuracy the cell average value is equivalent to the value at the cell centre, and so some method of approximating the values at the cell interfaces must be selected. As such, a FVM also requires one to specifiy a reconstruction scheme to extend these values stored at the cell centres to the cell edges to obtain the Riemann problem at that interface. A piecewise constant reconstruction where the cell average value is simply used at the interface is the simplest such scheme, but gives only first-order accuracy.

Second-order accuracy can be achieved by computing the gradient at each cell centre and using that to linearly extrapolate to the cell edges. However, this method generally gives rise to spurious oscillations in the resulting solutions, particularly near sharp flow features such as shock fronts. To counter this, most such schemes limit the gradient in areas of rapid change, reducing the local order of accuracy towards first-order. Such schemes are referred to as total variation diminishing (TVD) and various slope limiter functions such as those developed by Barth and Jespersen [9], Venkatakrishnan [10, 11], or Michalak and Gooch [12].

Therefore, it is desirable to use a scheme for which these terms are exactly balanced for an equilibrium stationary solution. Such a method has been developed by KM, termed a well-balanced scheme, and the salient results of their derivations are reproduced here.

1.2.3 Time Discretization

After spatial discretization, the system of equations (1.3) can be written in the semi-discrete form

$$\mathbf{U}_t = \mathbf{R}(\mathbf{U}), \tag{1.10}$$

where $\mathbf{R}$ is a simple notation to represent the residual from the chosen spatial scheme, as outlined above.

The time discretization which is then used to advance the solution is a four-stage, low-storage Runge-Kutta (RK) scheme with the following form

$$\begin{aligned} \mathbf{U}^{(0)} &\equiv \mathbf{U}^n, \\ \mathbf{U}^{(i)} &= \mathbf{U}^{(0)} + \beta_i \Delta t \mathbf{R}\left(\mathbf{U}^{(i-1)}\right), \qquad i = 1, \ldots, 4, \\ \mathbf{U}^{n+1} &\equiv \mathbf{U}^{(4)}, \end{aligned} \tag{1.11}$$

where n is the global time index and i is the index of the intra-timestep RK stage. The specific time-marching scheme used is described in [13] and has the coefficients

$$\beta_1 = 0.11, \quad \beta_2 = 0.2766, \quad \beta_3 = 0.5, \quad \beta_4 = 1. \tag{1.12}$$

Having $\beta_4 = 1$ ensures that such a scheme is consistent, and with $\beta_3 = 0.5$ the method is second-order accurate for both linear and non-linear equations. The values for β_1 and β_2 were designed to maxmize the CFL coefficient, and therefore possible timestep size, when paired with upwind based spatial discretization schemes. According to [14] and [15], having every $\beta_i \geq 0$ also means that the scheme belongs to the desirable class of strong stability preserving (SSP) RK methods.

Chapter 2

Simulation Results

2.1 Computational Environment

Simulations were carried out using the foam-extend 4.0 fork of the OpenFOAM (Open-Source Field Operation And Manipulation) software project.

2.2 Toy Problem

As previously mentioned, for an initial test of our well-balanced to the SASI, the simple toy model of FS [2, 3] was chosen. The salient details from those papers are reproduced here. Following the notation of FS, we will denote quantities in the supersonic region before the shock with a subscript "1", in the interior region between the shock and potential step with "in", and in the outflow region past the step with "out".

A schematic view of the problem domain can be seen in Fig. 2.1, showing how the overall scenario is split into two sub-problems for simulation. The entire test case consists of an supersonic inflow deccelerated at a stationary shock front, followed shortly after by a potential step which further slows the now subsonic flow. This provides a very simplistic analogue to study the mechanisms at play during the inflow, decceleration, and accretion of matter in a collapsing star before supernova.

For ease of simulation, the potential step and stationary shock are computed separately as sub-problems 1 and 2 respectively. This separation greatly simplifies the introduciton of specific advective and acoustic pertubations to appropriate locations in the interior of the domain, making it much easier to see the interactions of these disturbances at the boundaries (the shock and potential step) between the various flow regions.

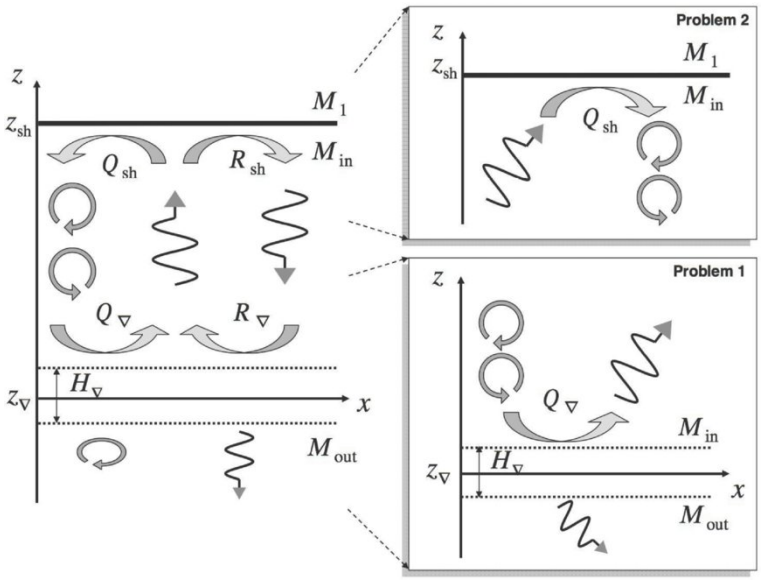

Figure 2.1: A short caption.

2.2.1 Sub-Problem 1

Description of potential step

2.2.2 Sub-Problem 2

Description of the standing shock

Bibliography

[1] John M. Blondin, Anthony Mezzacappa, and Christine DeMarino. Stability of standing accretion shocks, with an eye toward core-collapse supernovae. *The Astrophysical Journal*, 584(2):971–980, February 2003.

[2] Thierry Foglizzo. A simple toy model of the advective-acoustic instability. I. Perturbative approach. *The Astrophysical Journal*, 694(2):820–832, March 2009.

[3] Jun'ichi Sato, Thierry Foglizzo, and Sébastien Fromang. A simple toy model of the advective-acoustic instability. II. Numerical simulations. *The Astrophysical Journal*, 694(2):833–841, March 2009.

[4] Roger Käppeli and Siddhartha Mishra. Well-balanced schemes for the Euler equations with gravitation. *Journal of Computational Physics*, 259:199–219, February 2014.

[5] Sergei K. Godunov. A difference method for numerical calculation of discontinuous solutions of the equations of hydrodynamics. *Matematicheskii Sbornik*, 47(89):271–306, 1959.

[6] Philip L. Roe. Approximate Riemann solvers, parameter vectors, and difference schemes. *Journal of Computational Physics*, 43:357–372, October 1981.

[7] Viktor V. Rusanov. The calculation of the interaction of non-stationary shock waves and obstacles. *USSR Computational Mathematics and Mathematical Physics*, 1:304–320, March 1961.

[8] Eleuterio F. Toro, Michael Spruce, and William Speares. Restoration of the contact surface in the HLL-Riemann solver. *Shock Waves*, 4:25–34, July 1993.

[9] Timothy J. Barth and Dennis C. Jespersen. The design and application of upwind schemes on unstructured meshes. In *27th Aerospace sciences meeting*, page 366, January 1989.

[10] Venkat Venkatakrishnan. On the accuracy of limiters and convergence to steady state solutions. In *31st Aerospace Sciences Meeting*, page 880, January 1993.

[11] Venkat Venkatakrishnan. Convergence to steady state solutions of the Euler equations on unstructured grids with limiters. *Journal of Computational Physics*, 118(1):120–130, April 1995.

[12] Krzysztof Michalak and Carl Ollivier-Gooch. Limiters for unstructured higher-order accurate solutions of the Euler equations. In *46th AIAA Aerospace Sciences Meeting and Exhibit*, page 776, January 2008.

[13] Marie-Helene Lallemand. *Dissipative Properties of Runge-Kutta Schemes with Upwind Spatial Approximation for the Euler Equations*. PhD thesis, Rapport de Recherche 1179, INRIA Sophia-Antipolis, Valbonne, January 1990.

[14] Chi-Wang Shu and Stanley Osher. Efficient implementation of essentially non-oscillatory shock-capturing schemes. *Journal of Computational Physics*, 77(2):439–471, August 1988.

[15] Colin Barr Macdonald. Constructing high-order Runge-Kutta methods with embedded strong-stability-preserving pairs. Master's thesis, Theses (Dept. of Mathematics), Simon Fraser University, August 2003.

Eidgenössische Technische Hochschule Zürich
Swiss Federal Institute of Technology Zurich

Declaration of originality

The signed declaration of originality is a component of every semester paper, Bachelor's thesis, Master's thesis and any other degree paper undertaken during the course of studies, including the respective electronic versions.

Lecturers may also require a declaration of originality for other written papers compiled for their courses.

I hereby confirm that I am the sole author of the written work here enclosed and that I have compiled it in my own words. Parts excepted are corrections of form and content by the supervisor.

Title of work (in block letters):

Authored by (in block letters):
For papers written by groups the names of all authors are required.

Name(s):	**First name(s):**

With my signature I confirm that

- I have committed none of the forms of plagiarism described in the 'Citation etiquette' information sheet.
- I have documented all methods, data and processes truthfully.
- I have not manipulated any data.
- I have mentioned all persons who were significant facilitators of the work.

I am aware that the work may be screened electronically for plagiarism.

Place, date	**Signature(s)**

For papers written by groups the names of all authors are required. Their signatures collectively guarantee the entire content of the written paper.